

STAT

**Page Denied**

Next 1 Page(s) In Document Denied

ENGINEERING EXPERIMENT STATION  
of the Georgia Institute of Technology  
Atlanta, Georgia

PROGRESS REPORT NO. 4  
PROJECT NO. A-271

INVESTIGATION OF METHODS FOR MEASURING THE  
EQUIVALENT ELECTRICAL PARAMETERS OF QUARTZ CRYSTALS

By

DOUGLAS W. ROBERTSON, S. N. WITT, JR. and WILLIAM R. FREE

- o - o - o - o -

CONTRACT NO. DA-36-039-sc-71191

DEPARTMENT OF THE ARMY PROJECT NO. 3-24-02-072  
SIGNAL CORPS PROJECT NO. 867B

- o - o - o - o -

16 JANUARY 1957 TO 1 JUNE 1957

PLACED BY THE U. S. ARMY  
SIGNAL CORPS ENGINEERING LABORATORIES  
FORT MONMOUTH, NEW JERSEY

Progress Report No. 4, Project No. A-271

TABLE OF CONTENTS

	Page
I. PURPOSE . . . . .	1
II. ABSTRACT . . . . .	2
III. CONFERENCES AND PUBLICATIONS . . . . .	3
IV. INTRODUCTION . . . . .	4
V. EXPERIMENTAL WORK AND CIRCUIT STUDIES . . . . .	5
A. Crystal Measurements Standard . . . . .	5
1. Introduction . . . . .	5
2. Impedance Calibrations . . . . .	6
3. Experimental Crystal Measurement Data . . . . .	16
4. Theoretical Crystal Studies . . . . .	19
B. Power Measurements . . . . .	26
1. Introduction . . . . .	26
2. Prototype Power Meter . . . . .	29
3. R-F Power Measurements . . . . .	32
C. Experimental CI Meter . . . . .	37
1. Coaxial Crystal Parameter Bridge . . . . .	37
2. Experimental Oscillators . . . . .	42
VI. CONCLUSIONS . . . . .	47
VII. PROGRAM FOR NEXT QUARTER . . . . .	49
VIII. PERSONNEL . . . . .	50
IX. APPENDIX . . . . .	51
A. Addendum . . . . .	51
B. Admittance Characteristics of Measured Crystals . . . . .	51

This report contains 66 pages.

Progress Report No. 4, Project No. A-271

LIST OF FIGURES

	Page
1. Impedance Calibration Measurement Setup . . . . .	6
2. Comparison of Various Methods of Line Length Subtractions . . . . .	9
3. Bridge Measurements of 100-Ohm Termination . . . . .	11
4. Bridge Measurements of 200-Ohm Termination . . . . .	12
5. Admittance Meter Measurements of 100-Ohm Termination . . . . .	15
6. Present Laboratory Measurements Standard Setup . . . . .	17
7. Crystal Holder Characteristics of Crystal No. Fa-116 . . . . .	20
8. Holder Equivalent Circuit for Crystal No. Fa-116 . . . . .	21
9. Characteristics of Crystal No. Fa-116 at 245 Mc/sec. . . . .	23
10. Rectangular Admittance Plot of Characteristics of Crystal No. Fa-116 at 245 Mc/sec. . . . .	24
11. Assumed Equivalent Circuit of Crystal No. Fa-116 at 245 Mc/sec . . . . .	25
12. Thermistor Bridge Power Measuring System . . . . .	27
13. Prototype Power Meter . . . . .	30
14. Prototype Power Meter Schematic . . . . .	31
15. R-F Power Measurements . . . . .	33
16. Ambient Temperature Variations of One and Two Thermistor Configurations . . . . .	35
17. Ambient Temperature Variations of Prototype Bridge . . . . .	36
18. Capacitance Bridge Oscillator . . . . .	44

Progress Report No. 4, Project No. A-271

LIST OF APPENDIX FIGURES

	Page
A-1. Admittance Characteristics of Crystal No. Fa-57 . . . . .	52
A-2. Admittance Characteristics of Crystal No. Fa-59 . . . . .	53
A-3. Admittance Characteristics of Crystal No. Fa-89 . . . . .	54
A-4. Admittance Characteristics of Crystal No. Fa-91 . . . . .	55
A-5. Admittance Characteristics of Crystal No. Fa-92 . . . . .	56
A-6. Admittance Characteristics of Crystal No. Fa-103 . . . . .	57
A-7. Admittance Characteristics of Crystal No. Fa-104 . . . . .	58
A-8. Admittance Characteristics of Crystal No. Fa-105 . . . . .	59
A-9. Admittance Characteristics of Crystal No. Fa-116 . . . . .	60
A-10. Admittance Characteristics of Crystal No. Fa-117 . . . . .	61
A-11. Admittance Characteristics of Crystal No. Fa-118 . . . . .	62
A-12. Admittance Characteristics of Crystal No. Fa-82 . . . . .	63
A-13. Admittance Characteristics of Crystal No. Fa-83 . . . . .	64
A-14. Admittance Characteristics of Crystal No. Fa-40 . . . . .	65
A-15. Admittance Characteristics of Crystal No. Fa-44 . . . . .	66

Progress Report No. 4, Project No. A-271

LIST OF TABLES

	Page
I. COMPARISON BETWEEN MEASUREMENTS OBTAINED WITH THE STANDARD SYSTEM AND MEASUREMENTS SUPPLIED BY USASEL . . . . .	18
II. COAXIAL CRYSTAL PARAMETER BRIDGE MEASUREMENTS . . . . .	39
III. CHECK OF BRIDGE REPEATABILITY . . . . .	40
IV. CHECK OF BRIDGE SYMMETRY . . . . .	41
V. CRYSTALS OPERATED IN CAPACITIVE BRIDGE OSCILLATOR . . . . .	46

Progress Report No. 4, Project No. A-271

I. PURPOSE

The purpose of this project is threefold:

1. To study and investigate methods and techniques for measuring the equivalent electrical parameters of quartz crystal units in the frequency range of 150 to 300 mc/s, including:
  - (a) A means for directly measuring the power drive of a crystal unit,
  - (b) A simple and practical means of cancelling the capacitance of the crystal unit,  $C_0$ , at the test frequency, and
  - (c) A means of measuring the effective resistance of the crystal unit at the series resonant condition.
2. To accumulate data from the investigations of 1. above, with a view of utilizing the information for the development of a practical test method for the frequency range 150 to 300 mc/s which will make it possible to:
  - (a) Subject the crystal to any selected drive level between the limits of 0.2 and 4.0 milliwatts,
  - (b) Measure crystal resistance values between the limits of 20 and 200 ohms,
  - (c) Attain an accuracy of resistance measurement of  $\pm 5$  ohms or  $\pm 10$  per cent, whichever is greater, and
  - (d) Attain an accuracy of resonant frequency determination within  $\pm 0.001$  per cent of the series resonant frequency of the crystal unit.
3. To study and investigate means for establishing a laboratory measuring technique to be used as a standard for measuring the equivalent electrical parameters of quartz crystal units in the frequency range of 100 to 300 mc/sec.

**CONFIDENTIAL**

Progress Report No. 4, Project No. A-271

II. ABSTRACT

Further investigations of the calibration of various commercially available instruments for use with the Laboratory Standard Crystal Measurements System were conducted. None of the particular instruments which were investigated were sufficiently accurate for one percent overall accuracy.

A developmental system was used to obtain several admittance circle diagrams for each of 15 high frequency crystals over the frequency range from 140 to 455 mc/sec. The data were compared with measurements from other sources.

Initial investigations of the equivalent circuits of high frequency crystals based on the data from the Measurements Standard indicated that the presently used equivalent circuit does not entirely account for the crystal's behavior. This investigation did not progress sufficiently to provide definite conclusions.

A prototype thermistor-bridge power meter for measuring the r-f power dissipated in VHF quartz crystals was constructed and tested. Comparative measurements indicated the unit to be capable of measuring r-f power from 0.5 to 4.0 mw with an accuracy of  $\pm 5$  percent.

Impedance measurements made with the Coaxial Crystal Parameter Bridge in a passive arrangement indicated the bridge accuracy to be comparable with that of other available methods.

An experimental UHF capacitance bridge oscillator was constructed that displayed characteristics suitable for use with the coaxial bridge. Crystal controlled oscillations as high as 420 mc/sec were obtained with a modified version of this oscillator.

Progress Report No. 4, Project No. A-271

III. CONFERENCES AND PUBLICATIONS

Mr. W. B. Wrigley, Mr. D. W. Robertson and Mr. S. N. Witt, Jr. attended a conference at USASEL on March 18, 1957. The technical status of this project and the future courses of action were discussed. The immediate objectives as outlined under Chapter VI, "Program for Next Quarter," were agreed upon.

A paper entitled "Quartz Crystals Above 200 Megacycles" was presented by Mr. S. N. Witt, Jr. at the Atlanta Section meeting of the Institute of Radio Engineers on April 26, 1957. A paper entitled "Crystal Measuring Techniques Above 200 Mc/sec" was presented by Mr. S. N. Witt, Jr. at the Eleventh Annual Frequency Control Symposium held in Asbury Park, New Jersey, on May 9, 1957.

**CONFIDENTIAL**

Progress Report No. 4, Project No. A-271

IV. INTRODUCTION

This report actually covers an extended period of reduced activity for the 4-1/2-month period from 15 January 1957 to 1 June 1957. This extension, requested by USASEL, resulted from administrative delays in negotiating a 12-month extension of the present contract. It is expected that support for full effort will again be applied in July 1957.

Progress Report No. 4, Project No. A-271

V. EXPERIMENTAL WORK AND CIRCUIT STUDIES

A. Crystal Measurements Standard

1. Introduction

During this period, only a portion of the phases of development of the Crystal Measurements Standard were continued. The subsections previously titled "Stable Signal Generators," "Power Measurements," and "Detector Systems" are not included in this report since data previously reported indicated that the signal generator presently in use was satisfactory for immediate project needs and since further advancement in the study of power measurements and detector systems will require the purchase of various additional pieces of commercial equipment.

Principal efforts were directed toward investigations of calibration accuracies of various devices in current use. This study was greatly facilitated by the use of a large scale digital computer. The conclusion from this study is that the impedance and admittance bridges in current use do not provide sufficient accuracy to fulfill the purpose of the project. This, however, does not necessarily imply that the types of instruments involved are not satisfactory since the particular instruments which were used had been subjected to mistreatments of various kinds. Conclusions as to the potential accuracy of each instrument must await the purchase of new equipment.

Many crystal measurement runs were made on newly arrived crystals. Some of these measurements were compared with measurements obtained from other instruments. These measurements are, of course, subject to the calibration errors of the instruments used.

Progress Report No. 4, Project No. A-271

Some theoretical studies were made concerning the appropriate choice of equivalent electrical circuits for quartz crystals. These studies made use of laboratory measurements on various high frequency crystals. They were conducted primarily to determine the ability of the present measurements system to provide useful information about the quartz crystals.

2. Impedance Calibrations

Efforts to establish the sources and magnitudes of instrument errors were continued. In particular, large amounts of data were obtained on the Hewlett-Packard Model 803A VHF Bridge and the General Radio Type 1602-B Admittance Meter. These data consist of measurements made on General Radio 50-, 100-, and 200-ohm terminations which are assumed to be accurate to within one percent for impedance magnitude. Comparisons were made on the assumption that the impedance values of these terminations are exact.

A typical measurement setup is shown in Figure 1. The frequency calibration

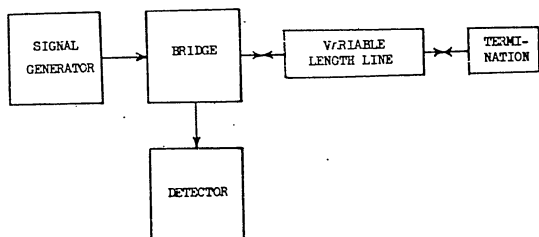


Figure 1. Impedance Calibration Measurement Setup.

Progress Report No. 4, Project No. A-271

of the Signal Generator was generally found to be satisfactory without the use of a frequency meter since no high-Q resonant elements are involved in the setup. The Variable Length Line consisted of assorted combinations of fixed-length air-dielectric transmission lines (General Radio) and in some cases included a constant-impedance adjustable line. Amplitude modulation of the signal source was sometimes employed to obtain greater useable detector sensitivity. This was also possible because of the absence of high-Q resonant elements in the setup. General Radio Type 874 connectors with "Cliplocks" were used in making coaxial connections wherever possible. Care was taken to reduce direct signal leakage between instruments to a minimum by minimizing non-critical line lengths and employing solid coaxial cable wherever possible.

Sources of errors which were discussed in the previous progress report are:

- a. human errors in reading the bridges,
- b. errors caused by poor null indication,
- c. drift in the bridge, terminations or other elements with time,
- d. errors in calibration of the terminations,
- e. errors inherent in the methods of applying corrections to the readings, and
- f. errors in bridge calibration.

Item e was the first of these sources of errors that was more fully investigated during this report period. Since impedance measurements were made for arbitrary lengths of transmission line, it was necessary to make one or more short-circuit measurements and then subtract the short-circuit impedance from the readings obtained when using the termination. Of the various possible methods of subtraction, the one making use of Z-Q charts or Smith charts

Progress Report No. 4, Project No. A-271

appeared to be most attractive because of the relatively small amount of time required. However, repetitive reduction of the same data yielded results differing by more than one percent in some cases. Mathematical subtraction of the short-circuit impedance using a slide rule was next attempted with a similar magnitude of disagreement resulting in the final impedance values. To obtain greater accuracy, a desk calculator and a set of mathematical tables were next employed. This combination was highly subject to human mistakes. The mistakes resulted primarily from the complexity of the computations. The equation which had to be solved was

$$Z_t = Z_o \frac{Z - \frac{Z_{sc}}{Z}}{Z_o - \frac{Z_{sc}}{Z}}$$

where  $Z_t$  is the impedance of the termination to be calculated from a bridge reading,

$Z_{sc}$  is the short-circuit bridge reading,

$Z$  is the bridge reading with the termination in place, and

$Z_o$  is the characteristic impedance of the transmission line.

Some of these quantities are complex impedances, thus adding to the difficulties already inherent in making the calculations.

Since satisfactory agreements were never obtained among the methods of short-circuit subtractions discussed above, the computations were performed on a Remington Rand EPA 1101 Univac Computer. Typical results obtained using the various computation methods are illustrated by Figure 2. It can be seen that the desk calculator calculations were sufficiently accurate, providing mistakes could be eliminated; however, this process was very time consuming, requiring

Progress Report No. 4, Project No. A-271

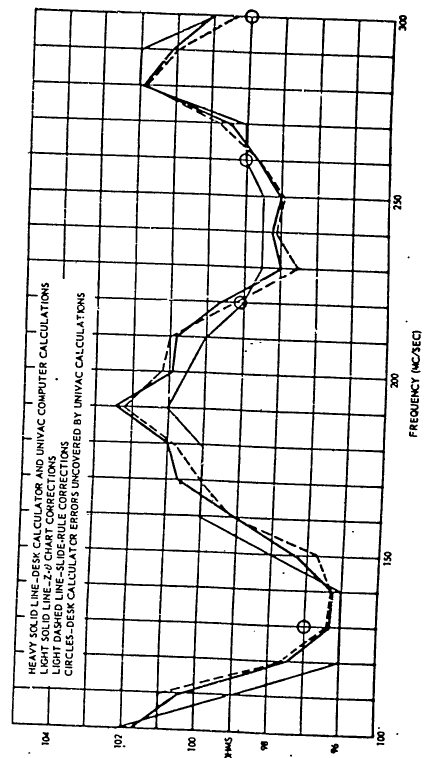


Figure 2. Comparison of Various Methods of Line Length Subtraction.



Progress Report No. 4, Project No. A-271

approximately 15 hours of time to subtract the short circuit for 20 points with the likelihood of appreciable errors remaining in 20 percent of the final solutions. The computer provided 0.01 percent accuracy with no mistakes in 43 seconds of computation time. Typical total computer time included 5 to 7 minutes program loading time plus 1 to 1.5 minutes per set of 20 readings for loading and computation. Fifteen to thirty minutes of personnel time were required for preparing the data for each set of 20 readings. The initial preparation of the computer program, however, required in excess of 20 hours of personnel time.

The use of the digital computer completely eliminated the errors inherent in the methods of applying corrections to the readings.

Figure 3 shows a graphical summary of the data obtained when using a particular HP Model 803A VHF Bridge to measure the impedance of a GR 100-ohm termination. Two of the curves show the data obtained by applying corrections for line length only. The third curve presents data which were fully corrected by applying the correction curves supplied with the bridge. These curves correspond to the curves of Figure 13 of Progress Report No. 3 except that the line length subtraction was performed by the computer for the current presentation. Some improvement in accuracy, especially for the phase angle, was obtained by the application of the correction curves provided with the bridge.

Figure 4 presents similar curves obtained by replacing the 100-ohm termination with a GR 200-ohm termination. An appreciable improvement in accuracy was obtained, in this example, by using the correction curves provided with the bridge. These curves correspond to Figure 14 of Progress Report No. 3.

Progress Report No. 4, Project No. A-271

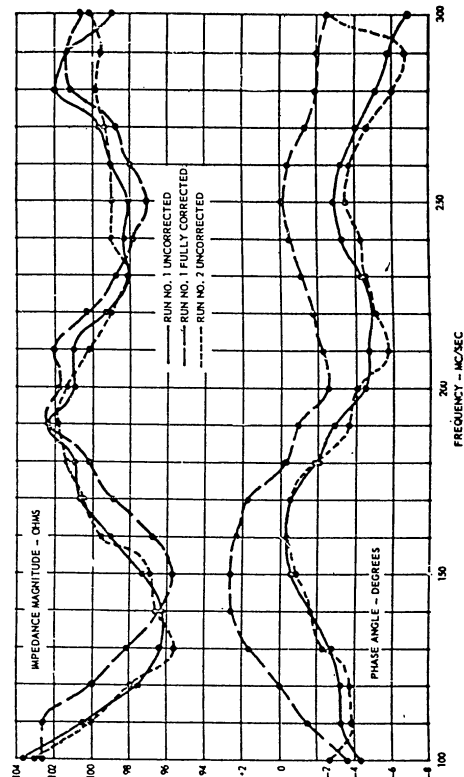


Figure 3. Bridge Measurements of 100-Ohm Termination.

**POOR ORIGINAL**

Progress Report No. 4, Project No. A-271

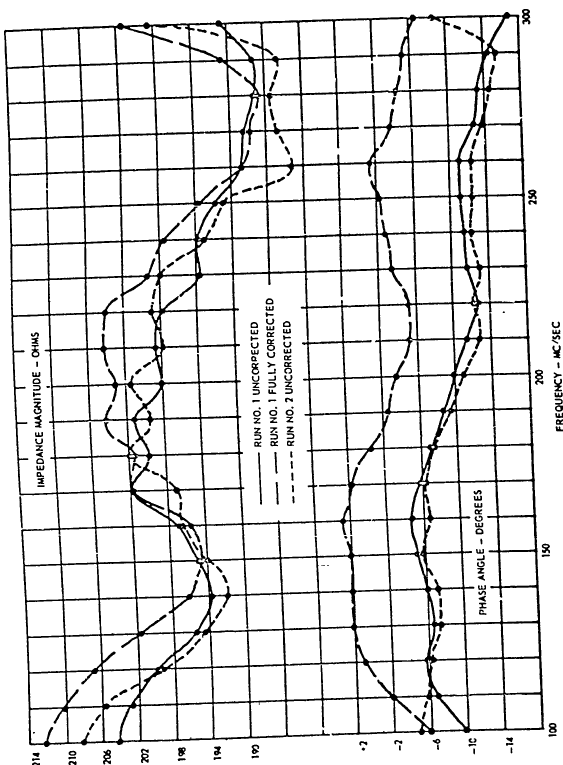


Figure 4. Bridge Measurements of 200-Ohm Termination.

Progress Report No. 4, Project No. A-271

Other data indicated that errors caused by poor null indication and errors due to drift were comparatively small for the previously presented data. Errors due to poor null indication may, however, become appreciable when AM modulation of the signal source cannot be used. Thus the errors indicated in Figures 3 and 4 may be associated with (1) human errors in reading the bridge, (2) errors in calibration of the terminations, and (3) errors in bridge calibration. The first and third errors may be appropriately grouped as "bridge errors." If the errors in calibration of the terminations can be considered to be zero, the data presented in Figures 3 and 4 indicate that the particular VHF bridge can be specified to be accurate to within 7 percent for impedance magnitude and within  $\pm 6$  degrees for phase angle with full corrections applied and for the particular impedances and line lengths involved. Other data indicate that approximately the same accuracy can be obtained for any impedance with a magnitude between 50- and 200-ohms and for a line length except lengths which approach odd multiples of one-quarter wavelength. The accuracy may be specified to be 9.5 percent for impedance magnitude and  $\pm 20$  degrees for phase angle when the computer is not used for short-circuit subtractions and when the corrections supplied with the bridge are not applied.

Another HP Model 803A VHF Bridge was briefly investigated and was found to have slightly poorer accuracy. Both of these bridges had been in use for several years and had not always received the proper treatment. This model of bridge has been improved by the manufacturer in recent years; thus, current production models may show appreciable improvement in accuracy over the particular instruments which were available to the project. Tentative plans are being made to either have one of the old bridges rebuilt or to purchase a new instrument for similar evaluation.

**POOR ORIGINAL**

Progress Report No. 4, Project No. A-271

The General Radio Type 1602-B Admittance Meter was also subjected to intensive laboratory investigations. Runs were made using 50-, 100-, and 200-ohm terminations separated from the instrument terminals by transmission line lengths of 0, 10, 20, 30, 40, and 50 cm. The computer program was modified to perform admittance subtractions based on short-circuit admittance readings. The difference in length of 0.6 cm between the short-circuit and the terminations was not included in the corrections; however, this distance would modify the results only slightly. If the instrument accuracy were greater, the correction for this distance would become more important. Figure 5 shows a graphical summary of the data obtained by using the 100-ohm termination. Near points where the line length approached one-quarter wavelength, large errors were to be expected. Disregarding these regions, however, the accuracy of the instrument can be specified in most cases to be within 15 percent for impedance magnitude. The curves show that the accuracy is generally greater for the shorter line lengths. For example, the maximum error in impedance magnitude for the 0-cm line length is 7.5 percent. The computer data gave phase angle accuracies within  $\pm 15$  degrees in most cases and a maximum error of 6 degrees for the 0-cm line length. This data is not presented graphically. Because of the large errors observed for the 100-ohm termination, it was felt that the use of the computer was not warranted for correcting the 50- and 200-ohm data. When the Admittance Meter is used with a half-wavelength line both magnitude and phase angle errors are greatly reduced (typically less than 5 percent magnitude error and less than  $\pm 4$  degrees phase angle error).

This particular Admittance Meter had been in use for several years and had received very rough treatment which probably accounts for much of the

Progress Report No. 4, Project No. A-271

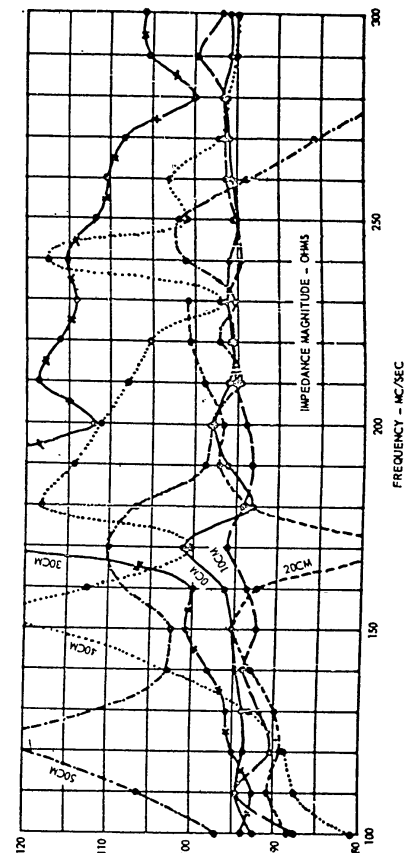


Figure 5. Admittance Meter Measurements of 100-ohm Termination.

CONFIDENTIAL

## Progress Report No. 4, Project No. A-271

error. Tentative plans are also being made to obtain a new Admittance Meter for evaluation.

It was concluded that the instruments presently in use do not even approach the accuracy required to satisfy the purpose of the project. The data indicate, however, that new instruments, if given special care in calibration, may be capable of providing the necessary accuracy. The possibility of including calibration data for a particular instrument in the computer program has also been suggested. As applied to crystal measurements, this would mean that the data obtained from the VHF Bridge or Admittance Meter would be placed into the computer and the resulting output would be the fully corrected impedance characteristics.

### 3. Experimental Crystal Measurement Data

Experimental data were obtained on a series of 15 high frequency quartz crystals supplied by the USASEL. Complete circle diagrams were obtained for the principal response at each overtone frequency between the frequency limits of 140 and 455 mc/sec for each crystal. The setup used for obtaining the diagrams is shown in Figure 6. This setup is identical to that presented in Figure 2 of Progress Report No. 3. Although the previous section indicated that the VHF Bridge may at present be made more accurate than the Admittance Meter, the Admittance Meter was chosen for the crystal measurements because of its requirement of less null detection sensitivity. A half-wavelength line was used for each measurement to obtain greater accuracy and so that line length subtractions would not be required. In all, 76 circle diagrams were obtained for the 15 crystal units. This number does not include the many minor responses (spurious) which were also obtained.

## Progress Report No. 4, Project No. A-271

The admittance characteristics of these crystals are shown in Figures A-1 through A-15 of the Appendix. Only the principal responses at each overtone are shown except for Figure A-15 where the frequency separations between the

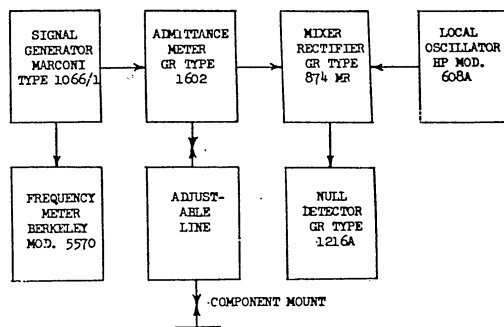


Figure 6. Present Laboratory Measurements Standard Setup.

principal responses and the spurious responses were very small. The numbers near each overtone response indicate respectively the overtone number and the approximate frequency of the response in mc/sec. The resonant frequency at each response is considered to be the frequency at the point of maximum conductance. This is the resonant frequency that would be obtained if cancellation coils were used to antiresonate the effective  $C_0$  of the crystal. The equivalent resistance is considered to be the reciprocal of the maximum

**POOR ORIGINAL**Progress Report No. 4, Project No. A-271

conductance. The reader is cautioned, however, that this method of  $C_0$  cancellation does not necessarily yield the resonant frequency of the motional arm of the crystal. This aspect is discussed in the next section of this report.

Table I shows a comparison between the resonant resistance and frequency obtained from the curves of Figures A-1 to A-15 and the corresponding data supplied by USASEL as obtained by using a Crystal Impedance Meter. The values of

TABLE I  
COMPARISON BETWEEN MEASUREMENTS OBTAINED WITH THE STANDARD SYSTEM AND MEASUREMENTS SUPPLIED BY USASEL.

Crystal No.	Standard Measurement System		Data from USASEL		$C_0$ ( $\mu\text{fd}$ )
	Frequency ( $\text{mc}/\text{sec}$ )	Resistance (ohms)	Frequency ( $\text{mc}/\text{sec}$ )	Resistance (ohms)	
Fa-57	144.997890	58	144.996591	60	7.1
Fa-59	144.995210	34	144.994504	38	6.6
Fa-89	154.969630	38	154.969724	38	5.8
Fa-91	155.025300	31	155.024304	32	5.8
Fa-92	154.963520	34	154.982208	35	5.8
Fa-103	165.010510	34	165.010252	36	6.4
Fa-104	164.965530	43	164.964807	42	6.0
Fa-105	164.950250	38	164.949722	37	5.9
Fa-116	175.029820	34	175.029814	36	4.8
Fa-117	174.899000	36	174.898072	33	5.7
Fa-118	174.896970	42	174.896575	39	5.8
Fa-82	188.944740	69	188.944609	70	6.1
Fa-83	188.996630	109	188.996369	102	4.4
Fa-40	195.979000	123	195.978463	106	6.0
Fa-44	196.013340	69	196.013830	63	8.1

Progress Report No. 4, Project No. A-271

$C_0$  as obtained by USASEL are also included. The effective  $C_0$  as determined by the Measurements Standard may be readily calculated by considering the value of the susceptance at the point of maximum conductance.

The maximum disagreement between resistance values is 14 percent. With two exceptions, the values agree within 9 percent and for 8 measurements the agreement is within 5 percent. In all cases, the frequencies agree to within better than 0.001 percent. In 3 cases, the frequency agreement is better than 0.0001 percent. The resistance disagreements do not appear to be related to the frequency disagreements except for the Crystal No. Fa-40 where the disagreements are large for both frequency and resistance. It is possible that the characteristics of this crystal may have changed somewhat between intervening measurements.

4. Theoretical Crystal Studies

One of the 15 crystals whose admittance characteristics are presented in the Appendix was examined in greater detail to determine the validity of the conventionally assumed equivalent electrical circuit. These studies and conclusions, while necessary to determine the usefulness of the Crystal Measurements Standard, are nevertheless subject to errors introduced by the present limited accuracy of the system. The particular crystal chosen for these studies was Crystal No. Fa-116 whose circle diagrams are shown in Figure A-9 of the Appendix.

The holder characteristic of Crystal No. Fa-116 was first determined. This was accomplished by using the measurement setup of Figure 6 for the frequency range from 100 to 1000  $\text{mc}/\text{sec}$ . The holder characteristic is plotted in Figure 7. The small circles represent the regions where crystal overtone

**POOR ORIGINAL**

Progress Report No. 4, Project No. A-271

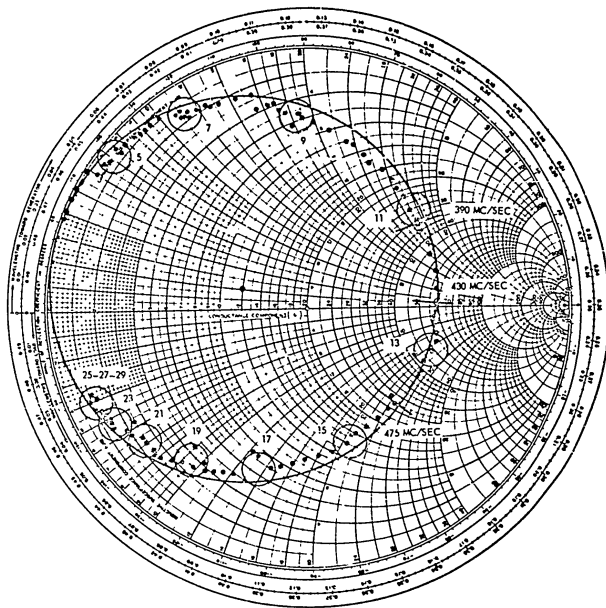


Figure 7. Crystal Holder Characteristics of Crystal No. Fa-116.

Progress Report No. 4, Project No. A-271

responses have a tendency to produce erroneous readings. The numbers near the small circles indicate the overtone number of the crystal response occurring in this region. The 21st through 29th overtone responses, all of which were appreciable and rather broad, made accurate readings difficult to obtain at frequencies above about 700 mc/sec. This situation was aggravated even more by the signal source instability at these frequencies (the crystal overtone responses at the higher frequencies have not been plotted due to this instability). The large circle in the figure was chosen as the circle which best represented the complete holder characteristic. It may be observed that this circle is not centered about the zero susceptance axis. This indicated the need for an additional shunt capacitance,  $C_o'$ , as a part of the holder equivalent circuit which is shown in Figure 8. The element values appearing in Figure 8 are the values calculated from the half-power points on the circle diagram of Figure 7. The value of  $(C_o + C_o')$  was also measured at 400 kc/sec and found to be 4.6  $\mu\text{fd}$ .

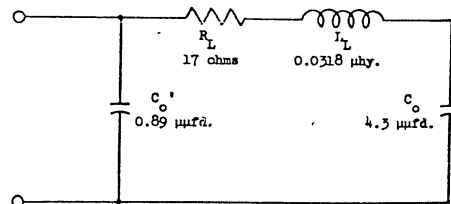


Figure 8. Holder Equivalent Circuit for Crystal No. Fa-116.

**COPY ORIGINAL**

Progress Report No. 4, Project No. A-271

The fact that the measured points on the holder characteristic follow an elliptical path indicated a slight nonlinearity of element values with frequency. However, this nonlinearity appears to be negligible. The elliptical shape may, moreover, be due entirely to measurement errors.

The crystal response at 245 mc/sec was chosen for detailed study. The measured points and the resulting circle approximation are described by Figure 9. Figure 10 presents the corresponding rectangular plot of the measured points. The assumed equivalent circuit of the crystal is shown in Figure 11. The resonant frequency of the crystal's motional arm could not be readily determined from the curves of Figures 9 and 10; however, the circle diagram of the motional arm was obtained by successive subtraction of the holder elements using admittance and impedance Smith charts. The shunt element,  $C_0$ , was first removed by displacing the circle as shown in Figure 9. The circle was next transferred to an impedance Smith chart (not shown) where  $L_1$  and  $R_1$  were removed. The circle was then transferred back to Figure 9 where  $C_0$  was removed as indicated. As would be expected, the center of the circle fell very nearly on the conductive axis. This fact, however, does not by itself substantiate the correctness of the assumed equivalent circuit. Various frequency points must also be investigated. For example, if the motional arm circle of Figure 9 is correct, its resonance must lie at the point  $F_0$ . If this point is traced back to the complete crystal diagram by use of the Smith chart transformations, it will occupy the various positions indicated. If the point,  $F_0$ , is transferred to Figure 10, it will not occupy the anticipated position. Time was not available before the preparation of this report to determine whether or not this is the normal frequency shift accompanying an impedance transformation.

Progress Report No. 4, Project No. A-271

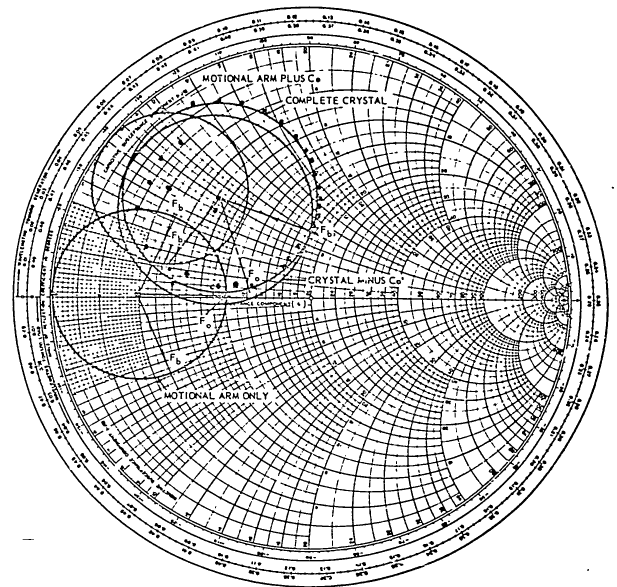


Figure 9. Characteristics of Crystal No. Fa-116 at 245 Mc/sec.

**CONFIDENTIAL**

Progress Report No. 4, Project No. A-271

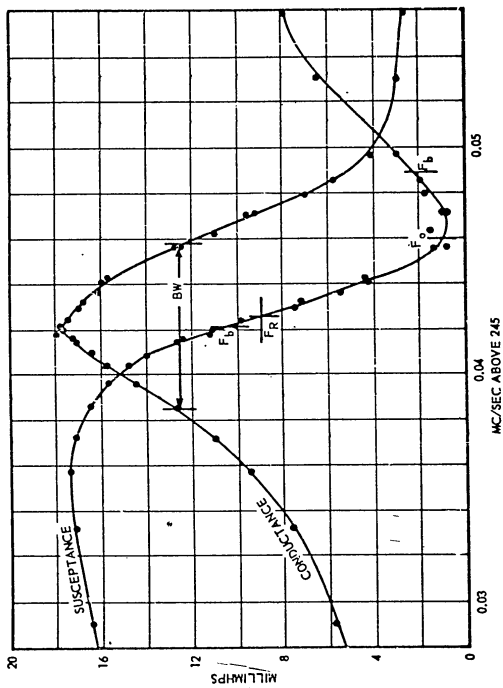


Figure 10. Rectangular Admittance Plot of Characteristics of Crystal No. Fa-116 at 245 Mc/sec.

Progress Report No. 4, Project No. A-271

If it is not, it is probable that the eventual explanation will result in the adoption of an alternate equivalent circuit.

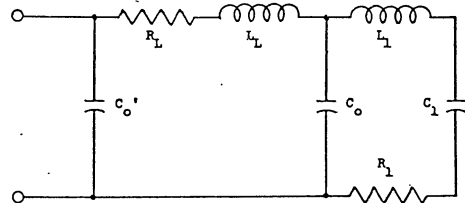


Figure 11. Assumed Equivalent Circuit of Crystal No. Fa-116 at 245 Mc/sec.

The element values for the equivalent circuit of the crystal's motional arm may also be determined by tracing the half-power bandwidth points,  $F_B$ , through the Smith charts to Figure 10, where the frequencies can be read from the curve. All natural and derived crystal parameters can then be calculated. For example, the  $Q_0$  of the motional arm was found to be 36,000. It is interesting to observe that the  $Q$  of the complete crystal unit with reactive cancellation may be calculated as 34,000 from Figure 10. It may also be observed from this figure that the most desirable reactive cancellation coil for this crystal unit would be one with a susceptance of 9 millimhos corresponding to an inductance of 0.07  $\mu$ h. This corresponds to an assumed  $(C_0 + C_0')$  of 5.85  $\mu$ fd, which, results in a crystal resonant frequency of 245.0426 mc/sec compared to the resonant frequency of the motional arm of 245.0450 mc/sec. This



**POOR QUALITY**

Progress Report No. 4, Project No. A-271

raises the question as to which frequency should be the basis for the specification of the crystal's parameters.

Although the above development did not progress sufficiently to provide definite conclusions, it did indicate the need for further study of the equivalent circuit of quartz crystals at high frequencies. It is probable that additional investigations will offer satisfactory explanations for some of the observations which have been cited or that errors may be found which will invalidate the results presented.

B. Power Measurements

1. Introduction

The equivalent electrical parameters of quartz crystals are to a varying extent a function of the crystal power dissipation, and it is therefore necessary to measure and specify the power level at which the parameters are measured. A power measuring device which is compatible with the developmental parameter measuring instrumentation should exhibit the following characteristics: (1) sufficient sensitivity to measure r-f power in the range from 0.2 to 4.0 mw, (2) the ability to measure r-f power over the frequency range from 150 to 300 mc/sec, (3) the ability to measure power without any electrical connection between the dissipating body and the power measuring device, and (4) the ability to measure the power dissipation of the crystal without access to the interior of the hermetically sealed can of the crystal unit.

A thermistor bridge r-f power measuring system of the type shown in Figure 12 shows the most promise of satisfying the above requirements. Presently available thermistors and null indicators make possible a system which is capable of exhibiting a sensitivity in excess of that necessary to measure

Progress Report No. 4, Project No. A-271

the power levels of interest. However, ambient temperature variations limit the degree to which this sensitivity can be practically utilized. The sensitivity of the system is limited by the maximum bridge unbalance indications which are caused by ambient temperature variations. These indications must be less than the allowable error of the minimum power level to be measured. The use of two thermistors in the bridge reduces the errors due to ambient temperature variations considerably, and makes possible the more effective utilization of the maximum sensitivity of the bridge.

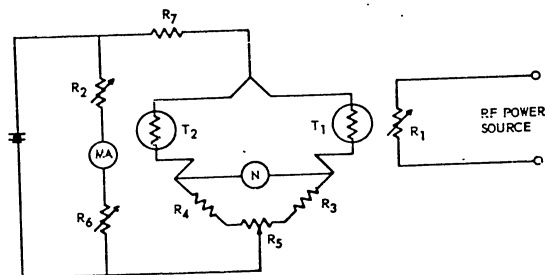


Figure 12. Thermistor Bridge Power Measuring System.

**POOR ORIGINAL**Progress Report No. 4, Project No. A-271

The two thermistors, shown as  $T_1$  and  $T_2$  on Figure 12, are mounted on the resistive elements of two rheostats,  $R_1$  and  $R_2$ , and are connected as adjacent arms of a wheatstone bridge. The bridge is balanced by adjusting the bridge balance potentiometer,  $R_5$ . The r-f power to be measured is applied to Rheostat  $R_1$ , causing the temperature of the rheostat to increase. This temperature increase is coupled to thermistor  $T_1$  and causes a decrease in the resistance of the thermistor. This decrease in the resistance of  $T_1$  causes an unbalance in the bridge. Applying d-c power to the second rheostat,  $R_2$ , causes the temperature of  $R_2$  and  $T_2$  to increase which in turn decreases the resistance of  $T_2$ . When the decrease in the resistance of  $T_2$  is equal to the decrease in resistance of  $T_1$ , the bridge will again be balanced. Under these conditions, the d-c power applied to  $R_2$  will be equal to the r-f power applied to  $R_1$ , provided the two rheostat-thermistor combinations are identical. Any errors introduced by differences in the two combinations may be easily determined by applying a known d-c power to  $R_1$  and adjusting the d-c power applied to  $R_2$  until the bridge is balanced. Any difference between the known d-c power into  $R_1$  and the d-c power applied to  $R_2$  represents the error due to differences in the two rheostat-thermistor combinations. Therefore, this difference between the two d-c powers may be used as a correction factor for the total system error.

The procedure described above makes possible the measurement of r-f power dissipation in a rheostat without any electrical connection between the rheostat and the power measuring instrument, thereby eliminating any possibility of the power measuring instrument altering the operation of the system containing the dissipating body.

Progress Report No. 4, Project No. A-271

The quartz slab of a conventional crystal unit is encased in a hermetically sealed can and it is impractical to insert a heat sensing element into the can of each crystal unit to be measured. If  $R_1$  is the rheostat of the Crystal Parameter Bridge or the test resistor used in the CI Meter substitution system, the r-f power dissipated in the rheostat will be equal to the r-f power dissipated in the crystal. Therefore, measurement of the power dissipated in the rheostat as described above, is equivalent to measurement of the power dissipated in the quartz crystal.

2. Prototype Power Meter

A prototype thermistor-bridge power meter for use in measuring the r-f power dissipated in VHF quartz crystals was constructed and tested. Figure 13 shows the prototype power meter connected to a Coaxial Crystal Parameter Bridge. A Minneapolis-Honeywell, Model 104WIG, Electronik Null Indicator is used as the null detector and a Marconi Type 1066/1 Signal Generator is shown connected as the r-f power source. A schematic diagram of the prototype power meter is shown in Figure 14. Two type 32CH Glennite Thermistors, shown as  $T_1$  and  $T_2$  on the schematic, were connected as adjacent arms of the bridge. The thermistors were bonded to the resistive films of two VHF Rheostats\* so that the temperature of the resistive films determines the temperature and, hence, the resistance of the thermistors. This bond was made with Sauereisen High Temperature Cement No. P-7

\* Robertson, D.W., Scott, T.R. and Wrigley, W.B., Investigation of Methods for Measuring the Equivalent Electrical Parameters of Quartz Crystals. Final Report, Contract No. DA-36-039-sc-56730, Georgia Institute of Technology, Atlanta, May 31, 1956, 11-31.

**POUR**

Progress Report No. 4, Project No. A-271

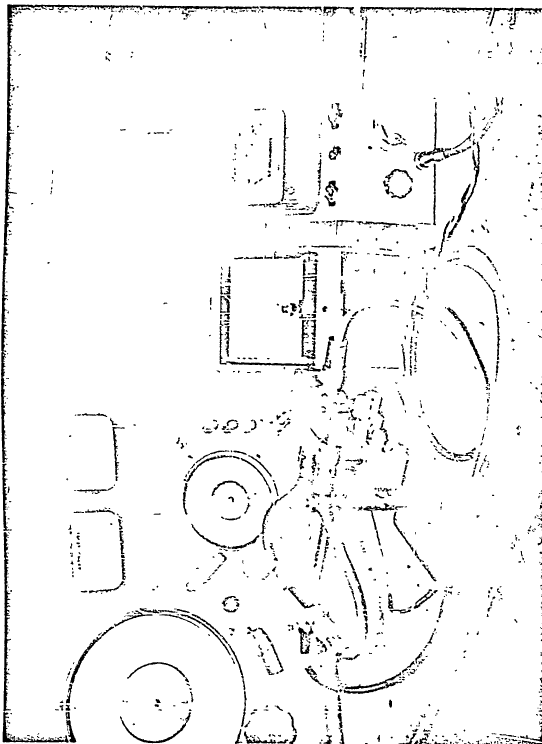


Figure 13. Prototype Power Meter.

Progress Report No. 4, Project No. A-271

which exhibits good heat conductivity and good electrical insulation. The test rheostat, shown as  $R_1$  on the schematic, is normally operated as the bridge rheostat in the Crystal Parameter Bridge or as the test resistor in the CI Meter substitution system. If the resistance of the test rheostat is equal to the

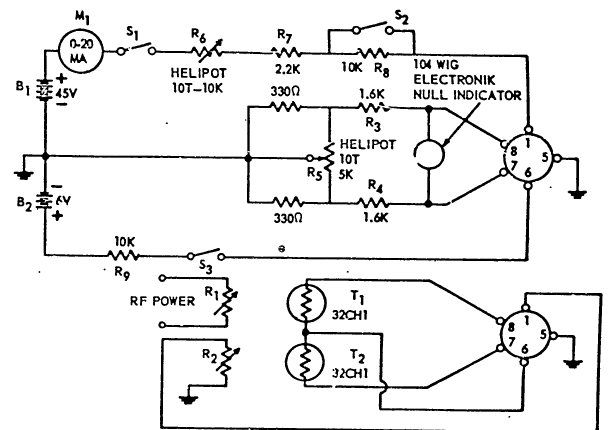


Figure 14. Prototype Power Meter Schematic.

**POOR QUALITY**

Progress Report No. 4, Project No. A-271

series resonant resistance of the quartz crystal under test and if the frequency is equal to the series resonant frequency of the crystal, the power dissipated in the test rheostat is equal to the power dissipated in the crystal. The reference rheostat,  $R_2$ , is mechanically connected to  $R_1$  to minimize ambient temperature variation effects. D-C power controlled by  $R_6$  and metered by  $M_1$  is dissipated in  $R_2$ .

The thermistor bridge is initially balanced with no power applied to the rheostats by adjusting  $R_5$  with the bridge d-c power on. The r-f power to be measured is then applied to  $R_1$ . The heat generated in  $R_1$  causes the resistance of thermistor  $T_1$  to decrease, unbalancing the bridge. D-C reference power is then applied to  $R_2$  and adjusted by  $R_6$  until the bridge is again balanced. The d-c power necessary to obtain this balance is read on  $M_1$ . This reference power, when corrected for system errors is equivalent to the r-f power in  $R_1$  and, hence, to the r-f power dissipated in the crystal.

3. R-F Power Measurements

In order to calibrate the power meter, specific amounts of d-c power ranging from 0.5 mw to 4.0 mw were applied to the test rheostat,  $R_1$ . The bridge was rebalanced by applying d-c reference power to the reference rheostat,  $R_2$ . The results are plotted as the d-c calibration curve of Figure 15. This curve represents the system error.

A Hewlett-Packard, Model 608C, VHF Signal Generator was used to apply specific amounts of r-f power, at 16 mc/sec, ranging from 0.5 mw to 4.0 mw, to  $R_1$ . The bridge was rebalanced by applying d-c reference power to  $R_2$ . The curve obtained from these r-f power readings is also shown in Figure 15 for comparison with the d-c calibration curve. The r-f power applied to the test rheostat was calculated from the HP Signal Generator attenuator dial reading.

Progress Report No. 4, Project No. A-271

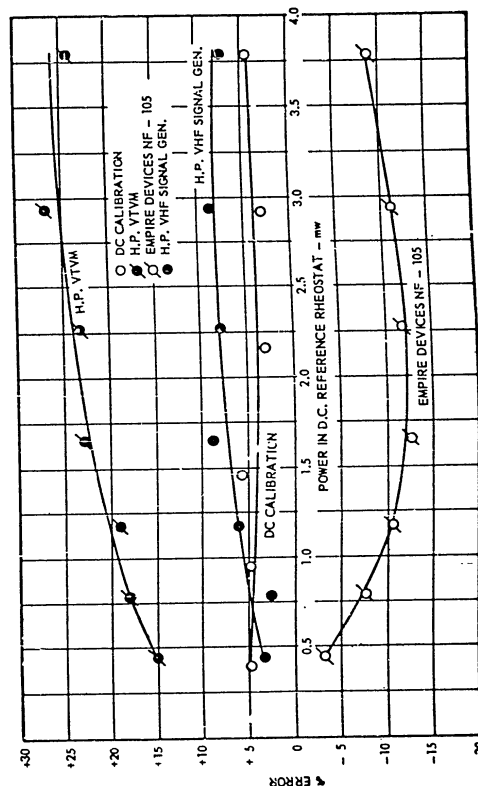


Figure 15. R-F Power Measurements.

**POUR LE JOURNAL**

Progress Report No. 4, Project No. A-271

In order to check the accuracy of the signal generator attenuator and as an additional check on the thermistor-bridge power meter, voltage measurements were made across the test rheostat with a Hewlett-Packard, Model 410B, Vacuum Tube Voltmeter and the signal generator output was measured with an Empire Devices, Model NF 105, Noise and Field Strength Meter. Results from these measurements are plotted on Figure 15 for comparison with the d-c power necessary in  $R_2$  to balance the thermistor bridge. Figure 15 does not give a true indication of the accuracy of the instruments compared because the power values were calculated by squaring the voltage readings obtained from the instruments and, therefore, the errors shown on the power curves are approximately twice the errors of the instruments. Hence, all three curves are within the accuracy claimed for the instruments involved.

Since the curve obtained with the Hewlett-Packard VHF Signal Generator lies approximately midway between the curves obtained with the voltmeter and field strength meter, the r-f powers calculated from the signal generator attenuator dial readings were taken as correct values of r-f power. With this assumption, a comparison between the d-c calibration curve and the HP VHF Signal Generator curve indicated that the prototype R-F Power Meter should be capable of measuring r-f power in the range from 0.5 mw to 4.0 mw with an accuracy of  $\pm 5$  percent.

Several termination type commercial r-f power meters appear to be sufficiently accurate for use in checking the prototype power meter. An attempt is being made to procure one or more of these units in order to further evaluate the accuracy of the thermistor bridge.

Progress Report No. 4, Project No. A-271

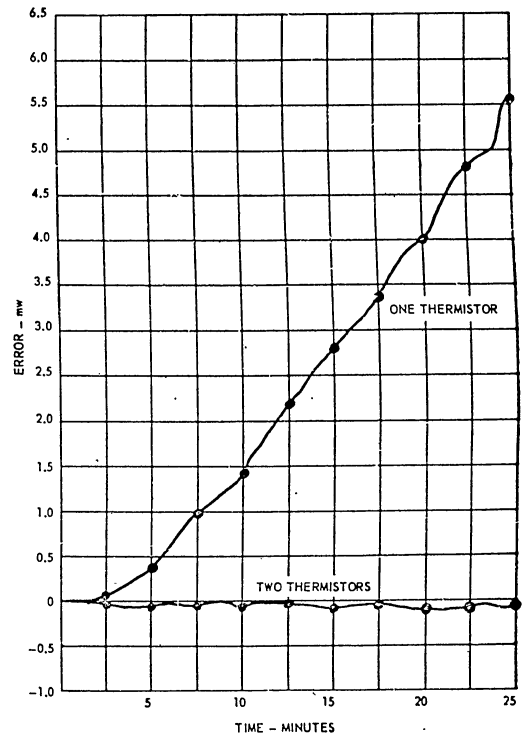


Figure 16. Ambient Temperature Variations of One and Two Thermistor Configurations.

POUR

Progress Report No. 4, Project No. A-271

In order to ascertain the improvement in useable bridge sensitivity obtained with two matched thermistors, tests were made over 30-minute periods with one-thermistor and two-thermistor bridge configurations. The results of these tests, as shown in Figure 16, indicated that the maximum error due to ambient temperature variations in the two-thermistor bridge was less than 2 percent of the error obtained with the one-thermistor bridge. Figure 17 shows the errors due to ambient temperature variations as a function of time in the two-thermistor bridge over a relatively long period of time. Assuming that a maximum period of 5 minutes is necessary to obtain a power reading, Figure 17

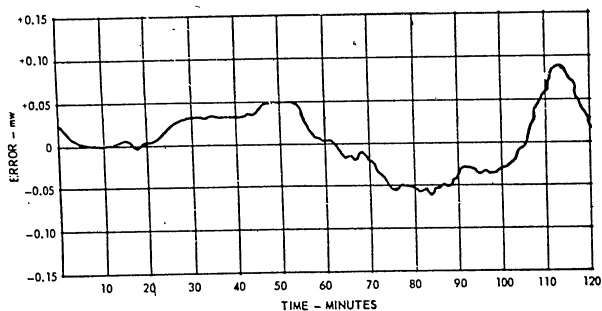


Figure 17. Ambient Temperature Variations of Prototype Bridge.

Progress Report No. 4, Project No. A-271

indicates that a maximum error of approximately 0.1 mw is possible. However, data from actual power measurements indicated that power levels as low as 0.5 mw could be consistently measured with an accuracy of  $\pm 5$  percent. The greater accuracy of the experimental readings was due to the improbability of the reading being taken at times when the temperature variations were maximum and to the fact that the time necessary to make the measurement was less than 5 minutes.

It is not possible, at the present time, to measure r-f power at a 0.2-mw level with the desired accuracy because the error due to ambient temperature variations is equivalent to a relatively large percentage of the r-f power being measured. Better matching of the two thermistors would reduce the deflections due to temperature variations and would permit lower values of r-f power to be measured with the desired accuracy. Improvement in the bonding between thermistor and dissipating body would result in a given ambient temperature deflection representing a smaller percentage of the power being measured and would also allow lower level r-f power to be measured accurately.

C. Experimental CI Meter

1. Coaxial Crystal Parameter Bridge

Progress Report No. 3 presented the results of passive measurements made on the Coaxial Crystal Parameter Bridge. These results indicated that the bridge in its present form was capable of matching impedances with errors of less than 15 percent in magnitude and less than 5 degrees in phase angle at drive levels as low as 0.5 mv. Considerably greater accuracy (5 percent and 2 degrees) was obtained by increasing the drive level or can be realized by increasing the sensitivity of the coupler elements. However, no effort was made to increase the sensitivity since the accuracy presently obtained is adequate to determine the usefulness of the bridge arrangement.

## Progress Report No. 4, Project No. A-271

Additional checks were made on the bridge by utilizing it in a passive measurement setup to measure the series resonant frequency and resistance of a number of crystal units furnished by USASEL. The resulting bridge measurements were compared with those obtained by USASEL and with those obtained at Georgia Tech with the present crystal measurement standard.

Figure 13 shows a picture of the passive system used. The Marconi 1066/1 Signal Generator which was used as the external signal source exhibited a short time stability that was more than adequate to permit proper bridge nulls to be obtained. The thermistor power meter, also shown in Figure 13, was not used to measure crystal drive because of the unavailability of VHF Rheostat-Thermistor units covering the entire frequency range of the group of crystals. However, the crystal drive was set at approximately 2 mw for each measurement by measuring the voltage across substitution resistors (approximately equal to  $R_1$ ) placed in each side of the coaxial bridge:

Table II compares the results of the bridge measurements with those obtained at USASEL and with those obtained with the Georgia Tech Crystal Measurements Standard. In each case a frequency difference of less than 0.001 percent, (target accuracy) was obtained between the bridge measurement and either of the two methods used for comparison. The average deviation appears to be approximately 0.0003 percent from the Measurements Standard and 0.0004 percent from the USASEL measurements.

Although resistance deviations greater than the desired accuracy of  $\pm 5$  ohms or 10 percent were obtained in four cases, these differences did not exceed 15 percent. With two of these crystals, No. Fa-40 and Fa-44, the differences occurred only between the coaxial bridge and the Measurements Standard results.

## Progress Report No. 4, Project No. A-271

With the other two crystals, No. Fa-57 and Fa-82, the coaxial bridge measurement differed from both the Measurements Standard and the USASEL results. However, caution should be exercised in the resistance comparisons since information was not available as to the conditions under which the USASEL resistance measurements were made and since the coaxial bridge results were obtained by measuring the VHF Rheostat resistances with a conventional ohm meter without regard to phase angle considerations.

TABLE II  
COAXIAL CRYSTAL PARAMETER BRIDGE MEASUREMENTS

Crystal No.	Coaxial Bridge		Measurements Stand.		USASEL	
	Frequency (mc/sec)	$R_1$ (ohms)	$\Delta f$ (percent)	$\Delta R_1$ (ohms)	$\Delta f$ (percent)	$\Delta R_1$ (ohms)
Fa-57	144.99760	52	+ .00020	+ 6	- .00068	+ 8
Fa-59	144.99511	33	+ .00007	+ 1	- .00040	+ 5
Fa-89	154.97008	36	- .00029	+ 2	+ .00023	+ 2
Fa-91	155.02555	30	- .00003	+ 1	- .00068	+ 2
Fa-92	154.98305	31	+ .00030	+ 3	- .00055	+ 4
Fa-103	165.00956	34	+ .00058	0	+ .00042	+ 2
Fa-104	164.96445	44	- .00065	- 1	+ .00021	- 2
Fa-105	164.94949	38	+ .00046	0	+ .00014	- 1
Fa-116	175.02918	34	+ .00037	0	+ .00035	+ 2
Fa-117	174.89883	37	+ .00010	- 1	- .00043	- 4
Fa-118	174.89625	39	+ .00041	+ 3	+ .00018	0
Fa-82	188.94369	61	+ .00055	+ 8	+ .00049	+ 9
Fa-83	188.99616	100	+ .00014	+ 9	+ .00002	+ 2
Fa-40	195.97879	110	+ .00011	+ 13	- .00017	- 4
Fa-44	196.01245	60	+ .00046	+ 9	+ .00070	+ 3

**POOR SIGNAL**

## Progress Report No. 4, Project No. A-271

To further check the usefulness of the bridge arrangement the consistency of the bridge was determined by repeating the measurements. Table III shows the results of two measurement runs, the second of which was performed one week after the first. As may be seen, the frequency differences were considerably less than 0.001 percent with only 5 of the 15 measurements exceeding 0.0005 percent. In addition all of the resistance values were well below the 5-ohm or 10-percent desired accuracy.

TABLE III  
CHECK OF BRIDGE REPEATABILITY

Crystal No.	Frequency (mc/sec)	$R_1$ (ohms)	$\Delta f$ (cycles)	$\Delta f$ (percent)	$\Delta R_1$ (ohms)
Fa-57	144.99760	52	+ 270	+ .00061	0
Fa-59	144.99511	33	+ 1306	+ .00069	+ 1
Fa-89	154.97008	36	+ 100	+ .00006	- 1
Fa-91	155.02535	30	- 530	- .00034	+ 3
Fa-92	154.98305	31	- 410	- .00027	+ 2
Fa-103	165.00956	34	- 350	- .00021	+ 2
Fa-104	164.96445	44	- 60	- .00003	0
Fa-105	164.94949	38	- 70	- .00004	+ 2
Fa-116	175.02918	34	+ 280	+ .00016	+ 4
Fa-117	174.89993	37	- 740	- .00042	+ 4
Fa-118	174.89625	39	+ 920	+ .00053	+ 2
Fa-82	188.94369	61	- 260	- .00014	+ 3
Fa-83	188.99636	100	- 1000	- .00053	- 2
Fa-40	195.97879	110	+ 620	+ .00032	- 5
Fa-44	196.01245	60	+ 1890	+ .00097	+ 1

## Progress Report No. 4, Project No. A-271

It was pointed out in Progress Report No. 3 that the major portion of the coaxial bridge error was due to the inherent unbalance of the basic bridge assembly. To further check this property the crystals were measured in both sides of the bridge and the results compared. These results are shown in Table IV. Although the frequency and resistance differences were small the bridge dissymmetry was verified by the consistent negative frequency and positive resistance errors.

TABLE IV  
CHECK OF BRIDGE SYMMETRY

Crystal No.	Frequency (mc/sec)	$R_1$ (ohms)	$\Delta f$ (cycles)	$\Delta f$ (percent)	$\Delta R_1$ (ohms)
Fa-57	144.99760	52	- 620	- .00043	+ 9
Fa-59	144.99511	33	- 250	- .00017	+ 5
Fa-89	154.97008	36	- 150	- .00029	+ 3
Fa-91	155.02535	30	- 270	- .00017	+ 2
Fa-92	154.98305	31	- 220	- .00014	+ 2
Fa-103	165.00956	34	- 600	- .00036	+ 3
Fa-104	164.96445	44	- 460	- .00028	+ 4
Fa-105	164.94949	38	- 400	- .00024	+ 6
Fa-116	175.02918	34	- 750	- .00043	+ 7
Fa-117	174.89883	37	- 1120	- .00065	- 4
Fa-118	174.89625	39	- 750	- .00043	+ 3
Fa-82	188.94369	61	- 60	- .00003	- 1
Fa-83	188.99636	100	+ 40	+ .00002	+10
Fa-40	195.97879	110	- 1390	- .00071	+10
Fa-44	196.01245	60	- 3040	- .00175	+ 2



BOOK REVIEW

Progress Report No. 4, Project No. A-271

The crystals were also measured in the coaxial bridge at their overtone frequencies in the 200- to 300-mc/sec frequency range. Since no USASEL measurements were available in this frequency range, the results were compared only with those obtained with the Crystal Measurements Standard. The frequency differences obtained were well below 0.001 percent in all but two questionable cases. However, considerable disagreement in resistance measurements was obtained, especially above 250 mc/sec. As of this report date an investigation of the possible causes of these discrepancies had not been made but additional measurements of crystal parameters and VHF Rheostat impedances are planned. A study of the bridge reaction to possible high frequency crystal equivalent circuits will also be made in an effort to determine the basic reasons for the resistance differences.

The results obtained with the coaxial bridge over the 100 to 200 mc/sec frequency range indicate that the presently obtainable accuracy is comparable with that of other available methods. In the 200- to 300-mc/sec range some question still remains as to the accuracy, particularly in respect to the crystal resistance measurements. Although additional efforts will be made to determine the causes of these resistance measurement discrepancies, the general accuracy and overall suitability are such that the bridge appears satisfactory for use in connection with the oscillator circuitry under development.

2. Experimental Oscillators

When the Crystal Parameter Bridge technique is used with an active oscillator, the frequency control is maintained by the crystal impedance variations near resonance as modified by the bridge configuration. In effect the crystal characteristic as presented to the oscillator is degraded by the shunt

Progress Report No. 4, Project No. A-271

arm of the bridge. In particular, a maximum impedance change of two to one is imposed, near bridge balance, by the variable rheostat of the shunt arm.

This impedance degradation, as discussed in Progress Report No. 3 is the major factor which prevented satisfactory operation of the Plate Degenerative Oscillator when used with the Coaxial Crystal Parameter Bridge. Additional experimental tests were made on this oscillator by utilizing passive elements in place of the crystal and bridge. These tests have confirmed the suspected inability of the Plate Degenerative Oscillator to oscillate satisfactorily with a maximum impedance change of only two to one. This was found to be true regardless of the phase angle considerations.

The bridge degrading property therefore necessitated an investigation of additional oscillatory circuitry which would not only meet the original requirements set forth in Progress Report No. 1 but would in addition be more sensitive to the phase and impedance changes exhibited by the bridge-crystal combination. Of the possible configurations only those which permitted one terminal of the crystal unit to be grounded and which permitted single capacitive neutralization of  $C_0$  were considered.

One configuration which appeared to meet these requirements was the capacitance bridge oscillator described in Progress Report No. 2. Two additional experimental models of this oscillator were constructed during the present report period. The construction of the first model which is shown schematically in Figure 18 was similar to that of the original in that it utilized a 2-in. hair-pin loop for the primary and a 1-in. loop for the secondary. These loops, however, were made physically wider in order to aid in reducing the cross coupling

## Progress Report No. 4, Project No. A-271

effects that were observed in the first model. A Faraday shield between the two loops was also utilized to prevent capacitive cross coupling. A Western Electric 417A tube which has a rated transconductance of 25,000 micromhos was used in the grounded grid amplifier. Crystal controlled oscillations could be obtained throughout the 200- to 300-mc/sec frequency range of the tuned circuit provided the  $C_o$  of each crystal used was individually neutralized.

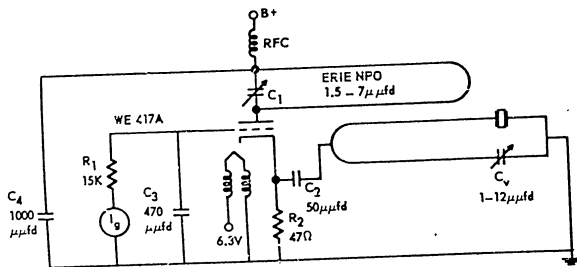


Figure 18. Capacitance Bridge Oscillator.

In order to determine qualitatively the sensitivity of the oscillator to the resonant characteristics of a bridge-crystal combination, a shunt resistance of 50 ohms was placed across the crystal. This resistor in effect simulated the degrading property that would be exhibited by the Coaxial Crystal Parameter

## Progress Report No. 4, Project No. A-271

Bridge. Under this condition crystal controlled oscillations could still be obtained throughout the 200- to 300-mc/sec frequency range.

In its present form two practical considerations prevent a further analysis of this circuit when used with the Coaxial Crystal Parameter Bridge. The first is the tuning capacitor  $C_1$  whose  $\frac{1}{2}$  turn of adjustment for the entire 200- to 300-mc/sec range makes tuning very difficult. The second is the physical arrangement which is such that the coaxial bridge cannot be conveniently connected in the circuit. It is contemplated that additional models will be constructed which will eliminate these two difficulties and permit a more complete analysis of the circuit to be made.

A second experimental model of this same basic configuration was constructed which utilized a modified Mallory UHF inductuner (shorted line) tunable from approximately 350- to 450-mc/sec. The modification consisted of placing two mirror image lines back to back in a manner such that mutual coupling could be obtained and such that both lines could be adjusted simultaneously. A copper foil Faraday shield was inserted between the lines and the oscillator components were mounted directly on the inductuner frame. The schematic diagram is essentially that of Figure 18 except a type 6AN4 tube was utilized and the tuning capacitor  $C_1$  was eliminated. Crystal controlled oscillations were obtained at frequencies as high as 420 mc/sec with this oscillator.  $C_o$  neutralization could be accomplished in most cases although the capacity required was considerably less than expected. Several crystals were tried with this oscillator and satisfactory operation was obtained in the majority of the cases. In particular the crystals of Table V were oscillated at the frequencies and overtones indicated. Complete  $C_o$  cancellation could not be obtained with Crystal

FOUR

Progress Report No. 4, Project No. A-271

effects that were observed in the first model. A Faraday shield between the two loops was also utilized to prevent capacitive cross coupling. A Western Electric 417A tube which has a rated transconductance of 25,000 micromhos was used in the grounded grid amplifier. Crystal controlled oscillations could be obtained throughout the 200- to 300-mc/sec frequency range of the tuned circuit provided the  $C_0$  of each crystal used was individually neutralized.

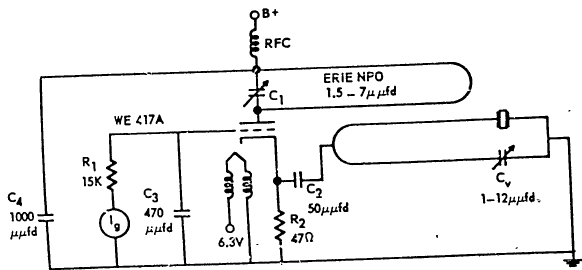


Figure 18. Capacitance Bridge Oscillator.

In order to determine qualitatively the sensitivity of the oscillator to the resonant characteristics of a bridge-crystal combination, a shunt resistance of 30 ohms was placed across the crystal. This resistor in effect simulated the degrading property that would be exhibited by the Coaxial Crystal Parameter

Progress Report No. 4, Project No. A-271

Bridge. Under this condition crystal controlled oscillations could still be obtained throughout the 200- to 300-mc/sec frequency range.

In its present form two practical considerations prevent a further analysis of this circuit when used with the Coaxial Crystal Parameter Bridge. The first is the tuning capacitor  $C_1$  whose  $\frac{1}{2}$  turn of adjustment for the entire 200- to 300-mc/sec range makes tuning very difficult. The second is the physical arrangement which is such that the coaxial bridge cannot be conveniently connected in the circuit. It is contemplated that additional models will be constructed which will eliminate these two difficulties and permit a more complete analysis of the circuit to be made.

A second experimental model of this same basic configuration was constructed which utilized a modified Mallory UHF inductuner (shorted line) tunable from approximately 350- to 430-mc/sec. The modification consisted of placing two mirror image lines back to back in a manner such that mutual coupling could be obtained and such that both lines could be adjusted simultaneously. A copper foil Faraday shield was inserted between the lines and the oscillator components were mounted directly on the inductuner frame. The schematic diagram is essentially that of Figure 18 except a type 6AN4 tube was utilized and the tuning capacitor  $C_1$  was eliminated. Crystal controlled oscillations were obtained at frequencies as high as 420 mc/sec with this oscillator.  $C_0$  neutralization could be accomplished in most cases although the capacity required was considerably less than expected. Several crystals were tried with this oscillator and satisfactory operation was obtained in the majority of the cases. In particular the crystals of Table V were oscillated at the frequencies and overtones indicated. Complete  $C_0$  cancellation could not be obtained with Crystal

**POUR LE PAVIL**

Progress Report No. 4, Project No. A-271

No. 1-3 at 355 mc/sec but lock-in oscillations were obtained.  $C_0$  cancellation was complete, however, from slightly above 355 mc/sec to well beyond the next overtone oscillation of this particular crystal which occurred at 400 mc/sec. Although very little is known at the present time regarding the frequency  $\epsilon$ -controlling properties of crystals at these overtones, it is of interest to note the position of these particular crystal responses on the Smith charts presented in the appendix. The proximity of these responses to the higher conductance portion of real axis appears to be significant and indicates the need of further investigation.

TABLE V  
CRYSTALS OPERATED IN CAPACITIVE BRIDGE OSCILLATOR

Crystal No.	Fundamental Frequency (mc/sec)	Oscillating Frequency (mc/sec)	Overtone
1-3	23.5	353	15
Fa-44	28	364	13
3-W	25	375	15
Fa-59	29	376	13
Pc-118	35	382	11
Fa-91	31	403	13
1-3	23.5	400	17
Fa-44	28	420	15

Progress Report No. 4, Project No. A-271

VI. CONCLUSIONS

Calibration data and actual crystal measurement data indicate that the best accuracy presently obtainable with the Crystal Measurements Standard is about 5 percent for impedance magnitude and  $\pm 4$  degrees for phase angle. This is obtained by using a General Radio Type 1602-B Admittance Meter with a half-wavelength transmission line between the meter and the crystal. This accuracy is possible only under ideal conditions and only for certain crystals. The accuracy is limited principally by the accuracy of the Admittance Meter. Because of the poor condition of the available Admittance Meter, a new instrument would probably give a considerable improvement in accuracy.

Investigations concerning the presently used crystal equivalent electrical circuit indicated that the circuit does not satisfactorily represent all crystals at high frequencies. In particular, the need for a capacitance,  $C_0'$ , directly across the pin of the crystal holder is indicated. This study did not progress sufficiently to assert definite conclusions concerning the other elements of the equivalent circuit.

Numerous measurements on actual high frequency crystals resulted in close frequency agreement between the Crystal Measurements Standard, the Coaxial Crystal Parameter Bridge and other measurement methods. Measurements of equivalent resonant resistance did not provide the agreement anticipated. Disagreements in both frequency and resistance can possibly be accounted for by the lack of standardization of the method of cancelling  $C_0$  with different measurement systems. Such standardization is practical only by first arriving at a satisfactory equivalent circuit.

Program Report No. 4, Project No. A-271

A comparison with other power measurements indicated the prototype thermistor-bridge power meter to be capable of measuring r-f power in the range from 0.5 mw to 4.0 mw with an accuracy of  $\pm 5$  percent. Better matching of the two thermistors and improvement in the bonding between the thermistor and dissipating body should permit lower values of r-f power to be measured with the desired accuracy.

An experimental capacitance bridge oscillator was constructed that demonstrated an ability to maintain crystal controlled oscillations under conditions similar to those imposed by the Coaxial Crystal Parameter Bridge. A modified physical arrangement which will accept the coaxial bridge will be required in order to fully determine the capabilities of this configuration. Crystal controlled oscillations were obtained with a similar configuration at frequencies as high as 420 mc/sec. The present inadequate knowledge of the frequency controlling properties of crystals at these overtones reveals the need for further investigation of the results obtained.

Program Report No. 4, Project No. A-271

VII. PROGRAM FOR NEXT QUARTER

Work during the next quarter will be a continuation of that reported in the preceding pages with emphasis on the following objectives:

1. perform additional tests of the prototype crystal power measuring system to determine its accuracy;
2. continue the investigation of oscillator circuits for use with the Coaxial Crystal Parameter Bridge;
3. procure and evaluate new GR admittance meters and HP UHF bridges for use in the Crystal Measurements Standard; and
4. investigate additional commercial equipment for use in the Crystal Measurements Standard.

Submitted by:

*Douglas W. Robertson*  
Douglas W. Robertson  
Project Director

Approved by:

*W. B. Wrigley*  
W. B. Wrigley, Head  
Communications Branch  
of the  
Physical Sciences Division

**POOR COPY**

Progress Report No. 4, Project No. A-271

VIII. PERSONNEL

Biographical sketches of the key technical personnel were included in Progress Reports No. 1 and 2. The time contributed by each during the present period is:

Douglas W. Robertson	Project Director	Full Time
Samuel M. Witt, Jr.	Research Engineer	2/3 Time
William R. Free	Asst. Research Engineer	Full Time
James E. Laue	Technical Assistant	1/2 Time

Progress Report No. 4, Project No. A-271

IX. APPENDIX

A. Addendum

Figure 15, page 33 of Progress Report No. 3, has been found to be in error. The scale on the  $R_1/R_2$  Ratio (abscissa) was inadvertently shifted two grid divisions. The first grid line should be labeled 0.5 rather than 0, the third line should be 1.0 instead of 0.5, 1.0 should be 1.5, etc. With the corrected scale, the K factor obtained for an  $R_1/R_2$  ratio of 1 is .675 (actual point) which corresponds very closely with the power ratios of Tables I and II (first bonding condition) of that report.

B. Admittance Characteristics of Measured Crystals

This section contains 15 figures. Refer to page v, LIST OF APPENDIX FIGURES, for a listing of the crystals that were measured.

**POOR ORIGINAL**

Progress Report No. 4, Project No. A-271

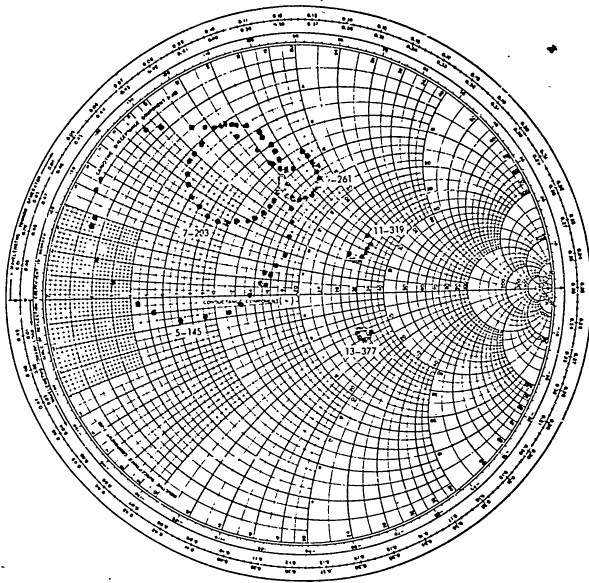


Figure A-1. Admittance Characteristics of Crystal No. Fa-57.

Progress Report No. 4, Project No. A-271

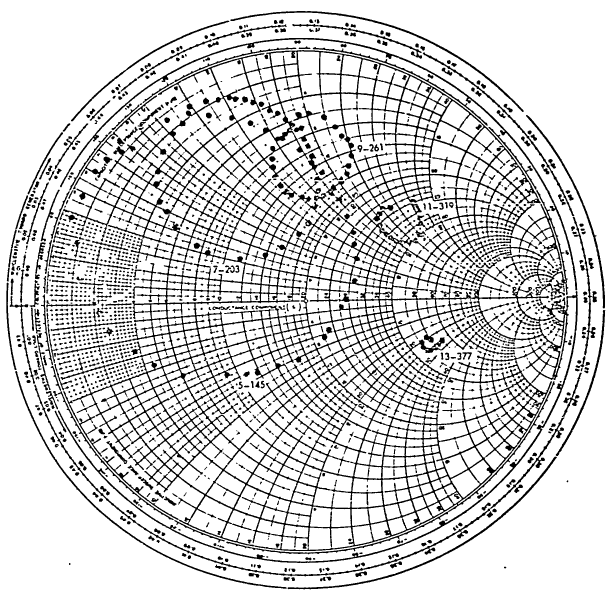


Figure A-2. Admittance Characteristics of Crystal No. Fa-59.

**POOR SIGNAL**

Progress Report No. 4, Project No. A-271

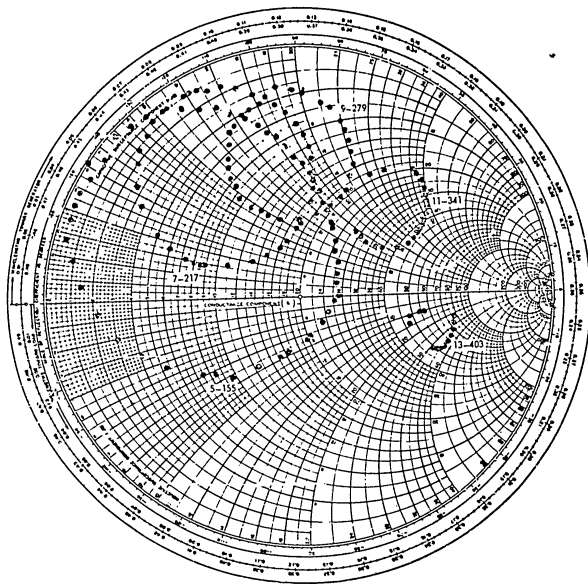


Figure A-3. Admittance Characteristics of Crystal No. Fa-89.

Progress Report No. 4, Project No. A-271

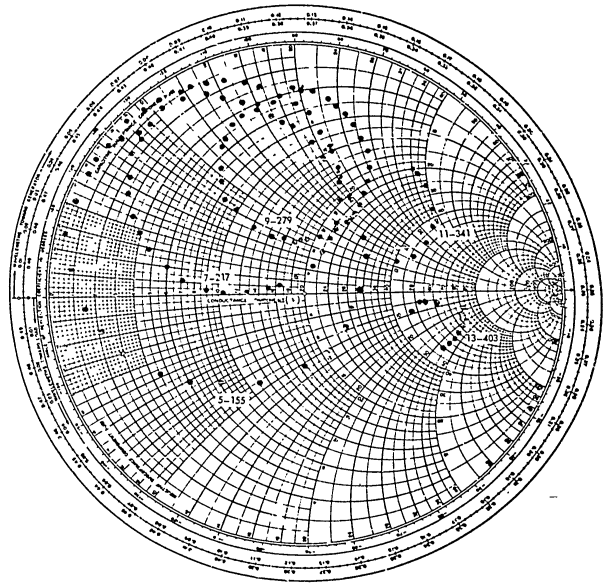


Figure A-4. Admittance Characteristics of Crystal No. Fa-91.



**POOR ORIGINAL**

Progress Report No. 4, Project No. A-271

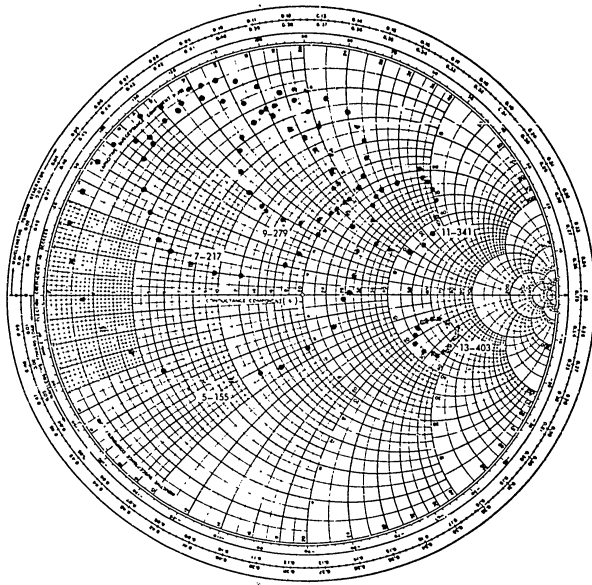


Figure A-5. Admittance Characteristics of Crystal No. Fa-92.

Progress Report No. 4, Project No. A-271

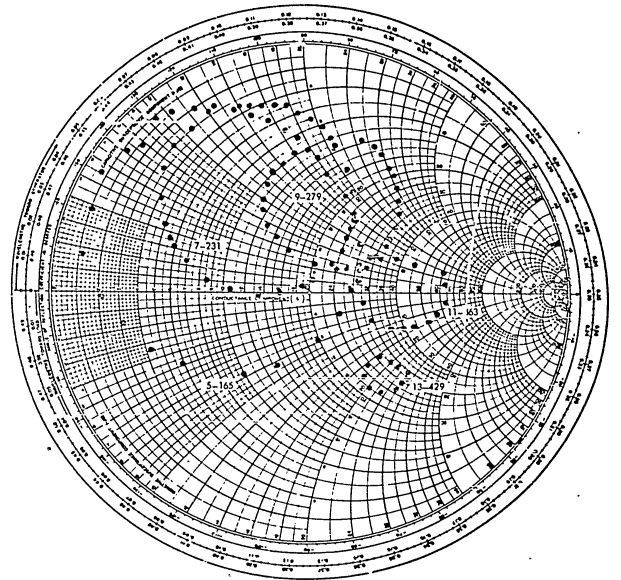


Figure A-6. Admittance Characteristics of Crystal No. Fa-103.

**POOR SIGNAL**

Progress Report No. 4, Project No. A-271

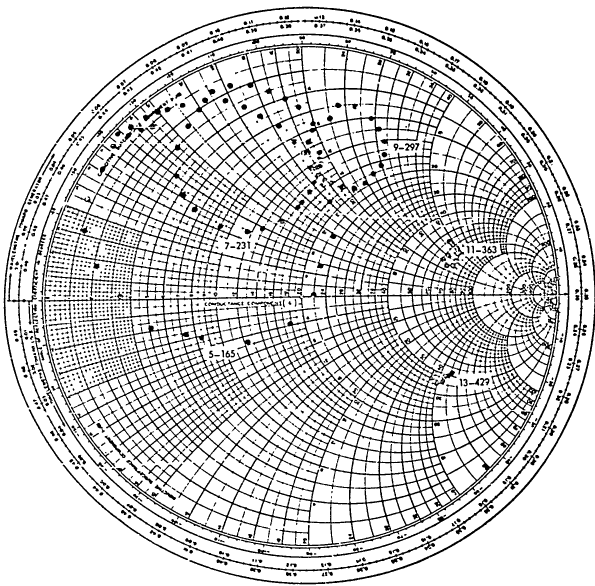


Figure A-7. Admittance Characteristics of Crystal No. Fa-104.

Progress Report No. 4, Project No. A-271

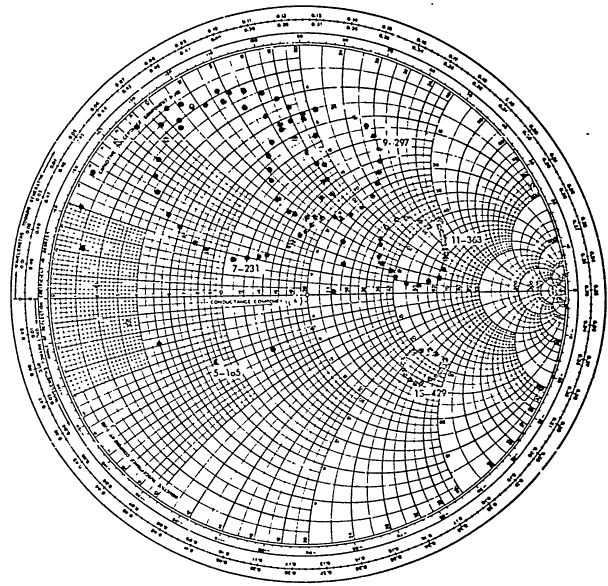


Figure A-5. Admittance Characteristics of Crystal No. Fa-105.

**POOR SIGNAL**

Progress Report No. 4, Project No. A-271

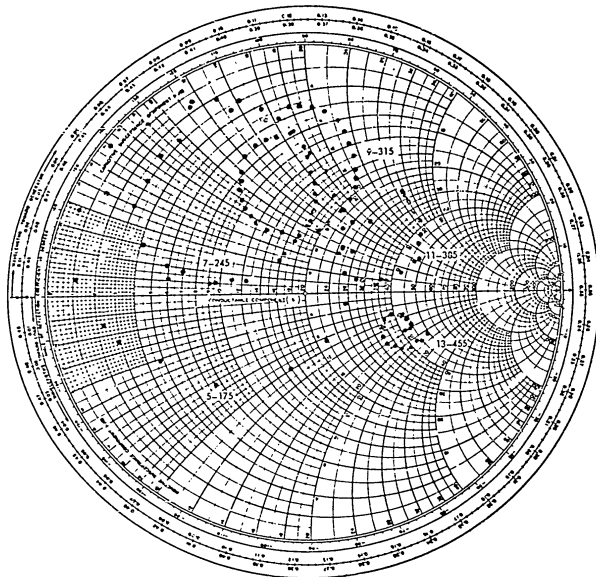


Figure A-9. Admittance Characteristics of Crystal No. Fa-116.

Progress Report No. 4, Project No. A-271

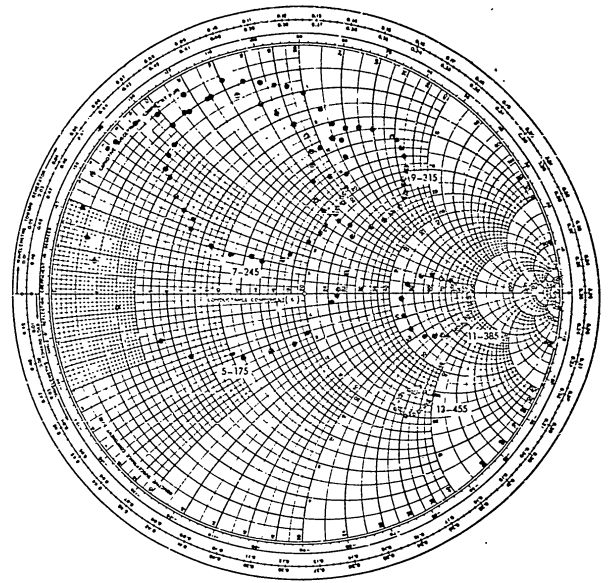


Figure A-10. Admittance Characteristics of Crystal No. Fa-117.

Progress Report No. 4, Project No. A-271

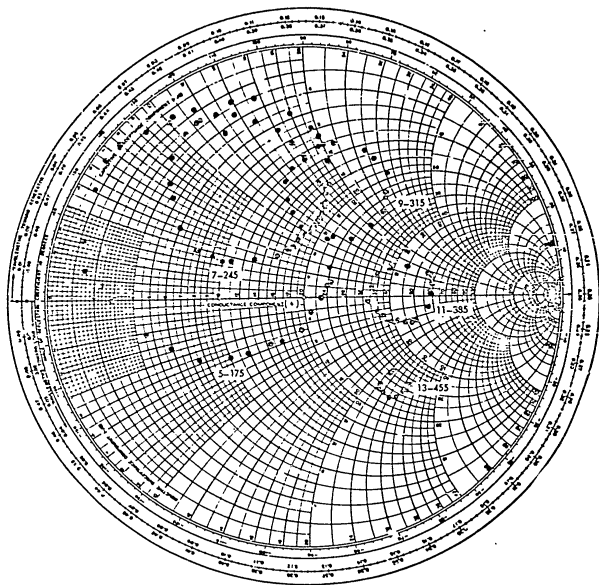


Figure A-11. Admittance Characteristics of Crystal No. Fa-118.

Progress Report No. 4, Project No. A-271

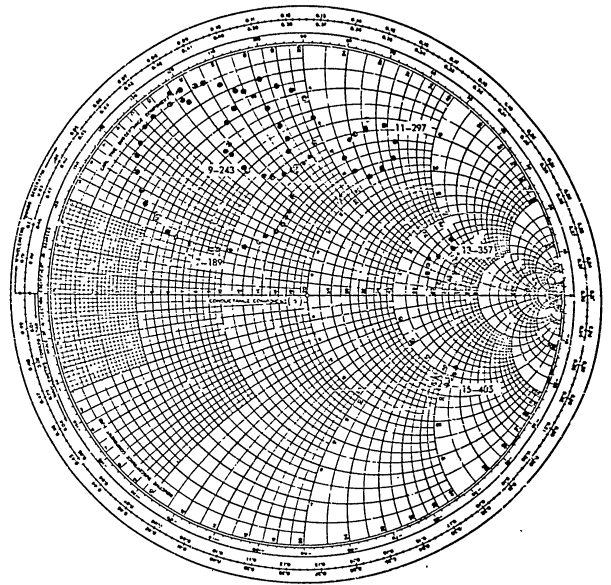


Figure A-12. Admittance Characteristics of Crystal No. Fa-82.

Progress Report No. 4, Project No. A-271

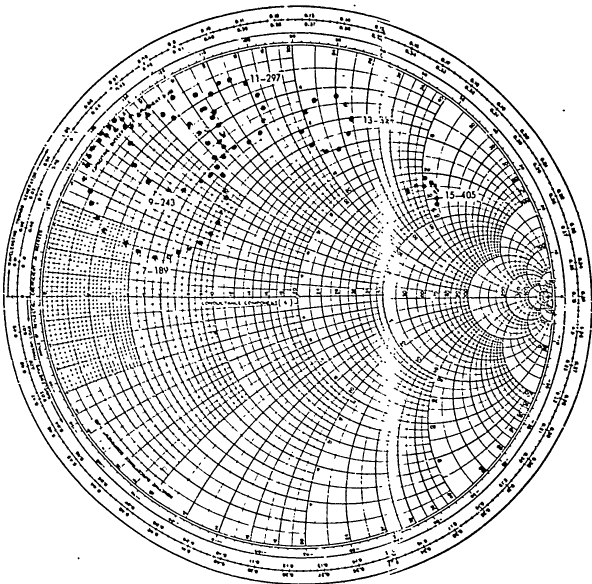


Figure A-13. Admittance Characteristics of Crystal No. Fa-83.

Progress Report No. 4, Project No. A-271

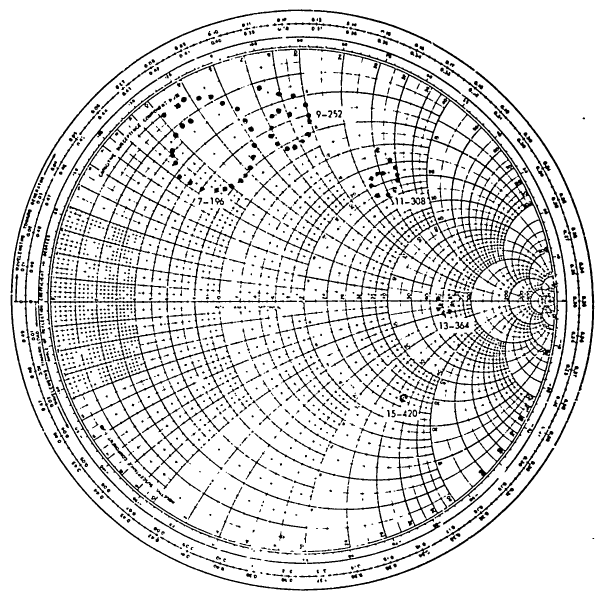


Figure A-14. Admittance Characteristics of Crystals No. Fa-40.

POOR QUALITY

Progress Report No. 4, Project No. A-271

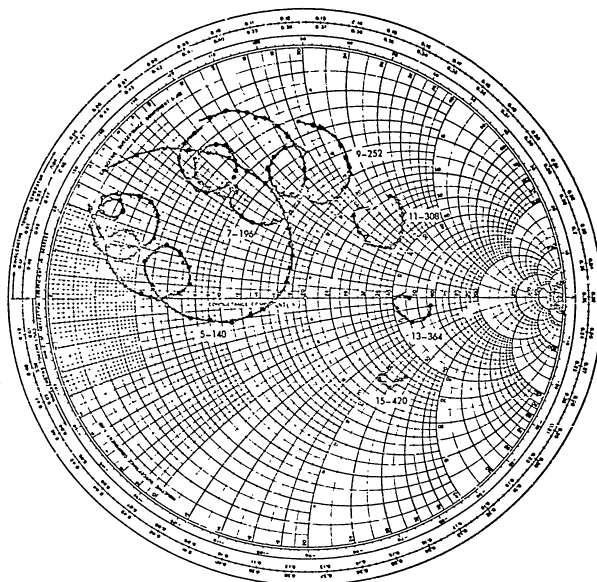


Figure A-15. Admittance Characteristics of Crystal No. Fa-44.

STAT

**Page Denied**